

***Ab initio* quasiparticle band structure of ABA and ABC-stacked graphene trilayers**Marcos G. Menezes,^{1,*} Rodrigo B. Capaz,¹ and Steven G. Louie^{2,3}¹*Instituto de Física, Universidade Federal do Rio de Janeiro, Caixa Postal 68528, 21941-972 Rio de Janeiro, Brazil*²*Department of Physics, University of California at Berkeley, Berkeley, California 94720, USA*³*Materials Sciences Division, Lawrence Berkeley National Laboratory, Berkeley, California 94720, USA*

(Received 13 September 2013; revised manuscript received 25 November 2013; published 27 January 2014)

We obtain the quasiparticle band structure of ABA and ABC-stacked graphene trilayers through *ab initio* density-functional theory (DFT) and many-body quasiparticle calculations within the *GW* approximation. To interpret our results, we fit the DFT and *GW* π bands to a low-energy tight-binding model, which is found to reproduce very well the observed features near the *K* point. The values of the extracted hopping parameters are reported and compared with available theoretical and experimental data. For both stackings, the self-energy corrections lead to a renormalization of the Fermi velocity, an effect also observed in previous calculations on monolayer graphene. They also increase the separation between the higher-energy bands, which is proportional to the nearest-neighbor interlayer hopping parameter γ_1 . Both features are brought to closer agreement with experiment through the self-energy corrections. Finally, other effects, such as trigonal warping, electron-hole asymmetry, and energy gaps, are discussed in terms of the associated parameters.

DOI: 10.1103/PhysRevB.89.035431

PACS number(s): 73.22.Pr, 71.15.-m

Graphene, a two-dimensional sheet of carbon atoms in a honeycomb lattice, has attracted a lot of attention of the scientific community in the last few years due to its unique electronic properties, which lead to several potential applications in nanoelectronics [1,2]. However, since graphene is a zero-gap semiconductor, much of the current effort is directed in finding ways to open a gap for use in electronic devices. In particular, one way to do that is to consider graphene stacks, where a number of layers are stacked on top of each other with a particular arrangement. Much work has been done on bilayer graphene, where it was found that a tunable gap can be opened through application of an external electrical field or through doping [3–6]. In light of recent experimental progress, graphene trilayers are also attracting increasing attention, revealing electronic properties that depend on the stacking order of the three layers. The two most important stackings are ABA (Bernal) and ABC (rhombohedral), which are shown in Fig. 1. For ABA stacking, the low-energy π bands are predicted to consist of a set of monolayer and bilayer-like bands, with linear and quadratic dispersions, respectively [2,7,8]. Therefore, this trilayer is expected to show mixed properties from these two systems, which were already observed experimentally [9]. In the presence of an external electrical field perpendicular to the layers, these bands hybridize and a tunable overlap between the linear and parabolic bands is introduced [10,11]. In contrast, for ABC stacking, the low-energy bands consist of a pair of bands with cubic dispersion, which are very flat near the Fermi level. The large density of states associated with this behavior indicates that many-body interactions might play a crucial role in this case. In fact, there are already a few works in the literature investigating the possibility of different competing phases in this system, such as ferromagnetic order [12], charge and spin-density waves, and quantum spin Hall phases [13], and even superconductivity [14,15]. Moreover, an external electrical field breaks the inversion

symmetry of this trilayer and induces a tunable band gap, in a similar fashion to bilayer graphene [7,11,16] and also observed experimentally [17,18]. We also point out that a similar type of dispersion and an associated quantum critical behavior were observed on a very different system, namely, the Laves phase of $\text{Nb}_{1+c}\text{Fe}_{2-c}$ [19,20].

In this work, we report first-principle calculations for ABA and ABC-stacked graphene trilayers, employing density-functional theory (DFT) [21,22] and many-body quasiparticle corrections within the *GW* approximation. Following the framework of Hybertsen and Louie [23], our calculations are done in two steps: First, a mean-field step is performed (DFT in our case), where the wave functions and energy bands are evaluated and stored. Then, in the next step, the quasiparticle corrections to the DFT energies are calculated within the *GW* approximation to the electron self-energy, by using the DFT energies and wave functions [24]. In our calculations, the DFT step is carried on using the local-density approximation (LDA) (Perdew-Zunger) approximation for the exchange-correlation functional [25], Troullier-Martins pseudopotentials for the electron-ion interaction [26], and a plane-wave basis set to expand the wave functions, with an energy cutoff of 60 Ry, as implemented in the QUANTUM ESPRESSO package [27]. The theoretical lattice constant for this pseudopotential is $a = 2.45 \text{ \AA}$ and the interlayer distance is set to the experimental value of graphite, $d = 3.35 \text{ \AA}$. We also use a vacuum region of 10.0 \AA in the direction perpendicular to the layers in order to avoid interaction between periodic images. In the second step, the many-body calculations are performed following the scheme described below, which is implemented in the BERKELEYGW package [28]. For the calculation of the dielectric matrix in reciprocal space, we use an energy cutoff of 9.0 Ry and a coarse 40×40 Monkhorst-Pack *K*-point sampling [29] with 200 unoccupied bands for general \mathbf{q} points away from zero and a fine 160×160 grid and 15 unoccupied bands for $\mathbf{q} \rightarrow 0$. This matrix is first evaluated in the static limit by using the random-phase approximation and then extended to nonzero frequencies by using a generalized plasmon pole model. The self-energy operator Σ is evaluated in the same

*marcosgm@if.ufrj.br

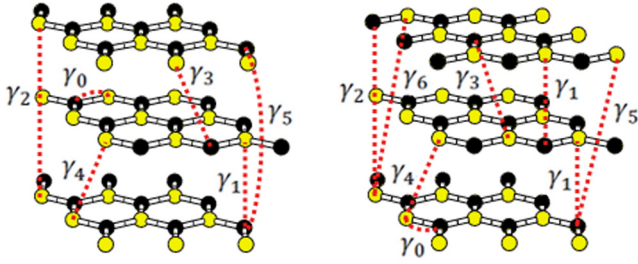


FIG. 1. (Color online) Arrangement of carbon atoms on the ABA (left) and ABC (right) graphene trilayers. Atoms belonging to the A and B sublattices of each layer are represented by yellow and black spheres, respectively. The red dashed lines indicate the tight-binding parameters included in the model used to fit our first-principles results (see text).

coarse grid. In this step, the Coulomb interaction is truncated in the middle of the vacuum region of the slab. Finally, the band-structure plots for the LDA and *GW* bands are generated along high-symmetry lines by using Wannier interpolation, as implemented in the WANNIER90 package [30].

The results of our calculations are shown in Fig. 2, where we compare the LDA and *GW* band structures in the energy range of the π bands. For both calculations, we see that the band structures share the same qualitative features. For ABA stacking (left), the band structure near the Fermi level consists of a superposition of a pair of nearly linear bands, resembling those of monolayer graphene, and two pairs of parabolic bands, resembling those of bilayer graphene. However, unlike single and bilayer graphene, both sets of bands have small band gaps, due to the lack of inversion symmetry (or, equivalently, A-B sublattice symmetry) in this trilayer. There is also a small offset between the linear and parabolic bands. The values of the gaps at the K point and energy offsets for LDA and *GW* are reported in Table I, where they are also compared with recent experimental data. The agreement is good, especially for the energy offset. The *GW* gaps are systematically larger than the corresponding LDA gaps, which

TABLE I. Energy gaps and energy offset (meV) of the monolayer and bilayer-like bands in the ABA-stacked trilayer. The offset is defined as the energy difference between the middle of the two gaps.

	LDA	<i>GW</i>	Exp. [9]
Monolayer gap	12	35	7
Bilayer gap	17	32	14
Offset	22	21	25

is a common trend observed in *GW* calculations [23], and they are also larger than the experimental values. Possible reasons for this discrepancy are the unavoidable residual doping and substrate effects present in experiments, which tend to enhance screening and decrease the quasiparticle gap. We also point out that, although the LDA gaps seem to agree well with the experimental values, such an agreement is only fortuitous. It is well known that DFT underestimates quasiparticle gaps, even if the exchange-correlation functional was known exactly [31]. Another important effect of the quasiparticle corrections is the renormalization of the Fermi velocity, which is visible from the increase of slope of the linear bands in *GW* when compared to LDA, a feature also observed in previous *GW* calculations in monolayer graphene [32–34].

For ABC stacking (right), the band structure is very different from the previous case. Near the Fermi level, there is a pair of bands with cubic dispersion, which are very flat near the K point. Moreover, in contrast with ABA, the ABC trilayer does have inversion symmetry, so the valence and conduction bands touch at the Fermi level. Due to the presence of a gap at the K point, these bands touch at three equivalent points located along the M - K lines, where the dispersion is roughly linear. Further away from the Fermi level, there are two pairs of parabolic energy bands.

Next, we fit the calculated *ab initio* π bands to a low-energy tight-binding (TB) model in order to extract the parameters that best describe the quasiparticle band structures. The hopping parameters included in our model are shown in Fig. 1, where the red dashed lines indicate the atoms connected by them. Atoms belonging to the inequivalent A and B sublattices are represented by yellow and dark spheres, respectively. Following common notation, γ_0 is the nearest-neighbor intralayer hopping and γ_1 is the nearest-neighbor interlayer hopping, connecting atoms that are right on top of each other in adjacent layers. These two parameters are sufficient to describe the main differences observed in the band structures, such as the type of dispersion of the low-energy bands and their separations. The other parameters, also shown in Fig. 1, describe finer details and follow from a generalization of the Slonczewski-Weiss-McClure (SWM) model of bulk graphite [35], and we use the same definition and sign convention for the parameters that are common to this model, which is extensively discussed in the literature [7–10,16]. Another parameter, δ , not shown in Fig. 1, corresponds to the onsite energy difference between nonequivalent carbon atoms: High-energy sites correspond to carbon atoms on top of each other (connected by the γ_1 hopping) and low-energy sites correspond to carbon atoms on top of hexagon centers in adjacent layers. Finally, we point out

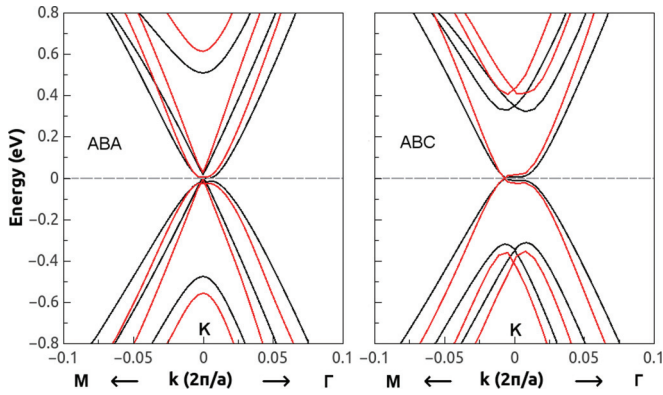


FIG. 2. (Color online) Comparison between the LDA (black lines) and *GW* (red lines) band structures obtained from our calculations for ABA (left) and ABC (right) stacking. The Brillouin-zone path is along the M - K - Γ directions from left to right, and it is centered in K . The Fermi level is set to zero in all cases, both in LDA and *GW*.

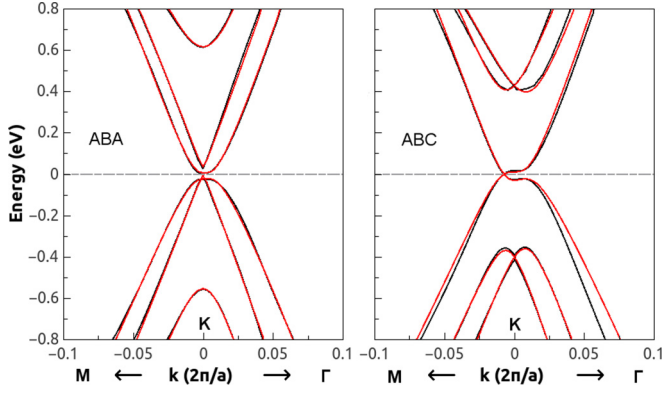


FIG. 3. (Color online) Comparison between the quasiparticle bands (black lines) and the corresponding adjusted TB bands (red lines) for ABA (left) and ABC (right) stacking. The path is the same as in Fig. 2, and the Fermi level is set to zero in both cases. Fitted parameters are shown in Table II.

that surface effects are neglected in our TB calculations, since they were found to be very small in previous calculations on the ABA trilayer [10].

We employ the least-squares method to fit the TB bands to either LDA or *GW* π bands from our calculations, thus obtaining the set of parameters that best describes them. Since we want to describe the details of the bands near the *K* point (such as the small energy gaps), only *K* points within a radius of $0.02 \, 2\pi/a$ from the *K* point are included in our fits. The comparison between *GW* bands and TB bands is shown in Fig. 3. We can see that the TB model describes very well the features observed in our calculations, even outside the radius of the fit. The fitted parameters are reported in Table II. Different sign conventions are used in the literature, so we explicitly indicate when a different convention is being used. For both stackings, the quasiparticle corrections increase the value of γ_0 , renormalizing the Fermi velocity ($v_0 = \sqrt{3}\gamma_0 a/2$) by about 28% in the ABA trilayer and 24% in the ABC trilayer, with respect to the LDA values. The *GW* value is in agreement with previous *GW* calculations on monolayer graphene [32–34]

and with the experimental value for the monolayer [36]. The parameter γ_1 , which is associated with the distance between the higher-energy bands and the Fermi level, is also increased by the quasiparticle corrections. In the absence of electron-hole asymmetry, these bands have energies $\pm\sqrt{2}\gamma_1$ for ABA and $\pm\gamma_1$ for ABC stacking at the *K* point [10].

We now discuss in detail the effects of the remaining TB parameters to the band-structure features. The parameter γ_3 causes a trigonal distortion of the low-energy bands. As can be seen in Fig. 3, in ABA stacking, the parabolic bands have four energy minima: one at the *K* point and three along the equivalent Γ -*K* lines. In our model, this is consistent with a positive sign for γ_3 [37], in agreement with bulk graphite and bilayer graphene. In ABC, γ_3 has a similar effect and is also positive, but there is an additional distortion caused by γ_2 , as we discuss below. The parameter γ_4 is responsible for a small electron-hole asymmetry in the bands. The ABA values for this parameter agree better with the experimental value from Bernal bilayer graphene than with the experimental value for this trilayer [5,9] (Table II). On the other hand, the ABC values appear to be overestimated, since the TB bands show a larger asymmetry than predicted by LDA and *GW*, especially outside the range of the fit. This could be related to an insensitivity of the fit to this parameter; that is, since γ_4 changes the curvature of the bands and they are mostly flat in the range of the adjustment, the curvature change may be not correctly reproduced outside that range.

The remaining parameters have quite different roles for each trilayer. For ABA stacking, the parameters γ_2 , γ_5 , and δ describe the inequivalency between A and B sublattices and are responsible for the opening of small band gaps in the linear and parabolic bands, also introducing an offset between them. As can be seen in Fig. 3, the TB model reproduces very well these features and the adjusted parameters are in good agreement with values from the literature. For ABC stacking, the parameter γ_2 also opens a gap between the cubic bands at the *K* point, but the presence of inversion symmetry prevents the full opening of a band gap in this case. Hence, γ_2 also induces a trigonal distortion, shifting the touching points of these bands from the *K* point to three points at the equivalent

TABLE II. Tight-binding parameters (in eV) obtained from our calculations (LDA or *GW* columns) and comparison with values from the literature, both theoretical and experimental. Wherever no value is shown, the corresponding parameter is either not applicable to that case or is set to zero. σ (in eV) is the standard deviation (error bars) of the adjustment inside its range.

Parameter	LDA	ABA <i>GW</i>	Exp. [9]	LDA	ABC <i>GW</i>	Theor. [16]	Bilayer exp. [5]	Graphite exp. [35]
γ_0	2.590	3.306	3.100 ^a	2.577	3.188	3.160 ^a	3.000 ^a	3.160
γ_1	0.348	0.414	0.390 ^a	0.348	0.415	0.502	0.400	0.390
γ_2	-0.043	-0.060	-0.028	-0.024	-0.041	-0.017	—	-0.020
γ_3	0.283	0.242	0.315 ^a	0.290	0.323	0.377 ^b	0.300 ^a	0.315
γ_4	0.162	0.152	0.041	0.196	0.287	0.099 ^b	0.150	0.044
γ_5	0.024	0.052	0.050	0.019	0.126	—	—	0.038
γ_6	—	—	—	0.004	0.084	—	—	—
δ	0.010	0.012	0.046	0.001	0.023	0.001 ^b	0.018	0.050 ^c
σ	0.002	0.006	—	0.002	0.006	—	—	—

^aThis parameter was not obtained in this reference; it was set to a value from the literature.

^bThe sign of this parameter was changed from the original reference in order to match our convention.

^c δ should not be confused with $\Delta = \delta + \gamma_2 - \gamma_5 = -0.008$ eV, a similar parameter used in graphite.

M - K lines. This is consistent with a negative sign for γ_2 in our model, in agreement with the ABA trilayer and graphite. On the other hand, the parameters γ_5 and γ_6 do not have any visible effects on the ABC band structure in the range considered, so they can be safely discarded in the description of the low-energy bands, as was done previously [16]. Nevertheless, we include in Table II the values given by the adjustment for future reference, but we stress that they could be also affected by insensitivity. Note that the ABC value for γ_5 cannot be directly compared with the values for ABA and graphite, since they have different definitions and roles. The parameter δ also plays a small role in the ABC trilayer, introducing only a small electron-hole asymmetry in a similar fashion to γ_4 . This could explain why the LDA value is smaller than the corresponding value for ABA, in agreement with the value obtained in a previous DFT calculation [16]. On the other hand, the GW value is larger than the corresponding ABA value, which could indicate either a larger asymmetry of the bands or again an insensitivity of the adjustment.

In conclusion, we have studied the quasiparticle band structure of ABA and ABC trilayer graphene within the GW approximation. The π bands obtained from these calculations were fitted to a TB model and the corresponding parameters were extracted. This model is found to reproduce very well the observed features in all cases, such as the type of dispersions and energy gaps. The fit parameters show a good agreement

with available data from graphene bilayers, trilayers, and graphite, and finer details of the bands are also correctly reproduced by them in the range of the fitting. The main effects of the quasiparticle corrections are the renormalization of the Fermi velocity and the increase of the separation between the higher-energy bands, where both bring theory to closer agreement with experiment. Therefore, we expect this work to provide future reference for studies on graphene trilayers and other stackings, which can reveal more interesting properties and applications.

ACKNOWLEDGMENTS

We thank Felipe Jornada for valuable discussions. This work was supported by the Brazilian funding agencies CAPES, CNPq, FAPERJ, and INCT-Nanomateriais de Carbono. Steven G. Louie acknowledges support from a Simons Foundation Fellowship in Theoretical Physics; from National Science Foundation Grant No. DMR10-1006184 (DFT and tight-binding analysis); and from the Director, Office of Science, Office Basic Energy Sciences, Materials Sciences and Engineering Division, US Department of Energy under Contract No. DE-AC02-05CH11231 (GW simulations). We also thank NERSC for the computational resources employed in our calculations.

-
- [1] K. S. Novoselov, A. K. Geim, S. V. Morozov, D. Jiang, Y. Zhang, S. V. Dubonos, I. V. Grigorieva, and A. A. Firsov, *Science* **305**, 666 (2004).
 - [2] A. H. C. Neto, F. Guinea, N. M. R. Peres, K. S. Novoselov, and A. K. Geim, *Rev. Mod. Phys.* **81**, 109 (2009).
 - [3] T. Ohta, A. Bostwick, T. Seyller, K. Horn, and E. Rotenberg, *Science* **313**, 951 (2006).
 - [4] Y. Zhang, T.-T. Tang, C. Girit, Z. Hao, M. C. Martin, A. Zettl, M. F. Crommie, Y. R. Shen, and F. Wang, *Nature Lett.* **459**, 820 (2009).
 - [5] L. M. Zhang, Z. Q. Li, D. N. Basov, M. M. Fogler, Z. Hao, and M. C. Martin, *Phys. Rev. B* **78**, 235408 (2008).
 - [6] E. V. Castro, K. S. Novoselov, S. V. Morozov, N. M. R. Peres, J. M. B. Lopes dos Santos, J. Nilsson, F. Guinea, A. K. Geim, and A. H. Castro Neto, *Phys. Rev. Lett.* **99**, 216802 (2007).
 - [7] F. Guinea, A. H. Castro Neto, and N. M. R. Peres, *Phys. Rev. B* **73**, 245426 (2006).
 - [8] B. Partoens and F. M. Peeters, *Phys. Rev. B* **74**, 075404 (2006).
 - [9] T. Taychatanapat, K. Watanabe, T. Taniguchi, and P. Jarillo-Herrero, *Nature Phys.* **7**, 621 (2011).
 - [10] M. Koshino and E. McCann, *Phys. Rev. B* **79**, 125443 (2009).
 - [11] B.-R. Wu, *Appl. Phys. Lett.* **98**, 263107 (2011).
 - [12] R. Olsen, R. van Gelderen, and C. M. Smith, *Phys. Rev. B* **87**, 115414 (2013).
 - [13] M. M. Scherer, S. Uebelacker, D. D. Scherer, and C. Honerkamp, *Phys. Rev. B* **86**, 155415 (2012).
 - [14] N. B. Kopnin, T. T. Heikkilä, and G. E. Volovik, *Phys. Rev. B* **83**, 220503(R) (2011).
 - [15] W. A. Muñoz, L. Covaci, and F. M. Peeters, *Phys. Rev. B* **87**, 134509 (2013).
 - [16] F. Zhang, B. Sahu, H. Min, and A. H. MacDonald, *Phys. Rev. B* **82**, 035409 (2010).
 - [17] C. H. Lui, Z. Li, K. F. Mak, E. Cappelluti, and T. F. Heinz, *Nature Phys.* **7**, 944 (2011).
 - [18] L. Zhang, Y. Zhang, J. Camacho, M. Khodas, and I. A. Zaliznyak, *Nature Phys.* **7**, 953 (2011).
 - [19] B. P. Neal, E. R. Ylvisaker, and W. E. Pickett, *Phys. Rev. B* **84**, 085133 (2011).
 - [20] A. Alam and D. D. Johnson, *Phys. Rev. Lett.* **107**, 206401 (2011).
 - [21] P. Hohenberg and W. Kohn, *Phys. Rev.* **136**, B864 (1964).
 - [22] W. Kohn and L. J. Sham, *Phys. Rev.* **140**, A1133 (1965).
 - [23] M. S. Hybertsen and S. G. Louie, *Phys. Rev. B* **34**, 5390 (1986).
 - [24] This one-step procedure is known as a “ G_0W_0 ” or a “one-shot” GW calculation. For more details, see Ref. [23].
 - [25] J. P. Perdew and A. Zunger, *Phys. Rev. B* **23**, 5048 (1981).
 - [26] N. Troullier and J. L. Martins, *Phys. Rev. B* **43**, 1993 (1991).
 - [27] P. Giannozzi *et al.*, *J. Phys.: Condens. Matter* **21**, 395502 (2009).
 - [28] J. Deslippe, G. Samsonidze, D. A. Strubbe, M. Jain, M. L. Cohen, and S. G. Louie, *Comput. Phys. Commun.* **183**, 1269 (2012).
 - [29] H. J. Monkhorst and J. D. Pack, *Phys. Rev. B* **13**, 5188 (1976).
 - [30] A. A. Mostofi, J. R. Yates, Y.-S. Lee, I. Souza, D. Vanderbilt, and N. Marzari, *Comput. Phys. Commun.* **178**, 685 (2008).
 - [31] R. M. Martin, *Electronic Structure: Basic Theory and Practical Methods* (Cambridge University Press, New York, USA, 2004).
 - [32] C.-H. Park, F. Giustino, C. D. Spataru, M. L. Cohen, and S. G. Louie, *Nano Lett.* **9**, 4234 (2009).

- [33] L. Yang, J. Deslippe, C.-H. Park, M. L. Cohen, and S. G. Louie, *Phys. Rev. Lett.* **103**, 186802 (2009).
- [34] P. E. Trevisanutto, C. Giorgetti, L. Reining, M. Ladisa, and V. Olevano, *Phys. Rev. Lett.* **101**, 226405 (2008).
- [35] M. S. Dresselhaus and G. Dresselhaus, *Adv. Phys.* **30**, 139 (1981).
- [36] Y. Zhang *et al.*, *Nature (London)* **438**, 201 (2005).
- [37] Note that it is common to find an opposite sign convention for γ_3 in the literature [9, 10, 16], so care must be taken when comparing results and using reference values. A discussion of the conventions and their relation to the SWM model can be found in Ref. [8].